NIH Public Access
Author Manuscript
J Magn Reson Imaging. Author manuscript; available in PMC 2014 July 09.

Published in final edited form as:
J Magn Reson Imaging. 2012 January ; 35(1): 72–78. doi:10.1002/jmri.22652.

Accuracy of MRI to Identify the Coronary Artery Plaque: A Comparative Study With Intravascular Ultrasound

Yi He, MD[1], **Zhaoqi Zhang, MD**[1,*], **Qinyi Dai, MD**[1], **Yujie Zhou, MD**[2], **Ya Yang, MD**[3], **Wei Yu, MD**[1], **Jing An, MS**[4], **Lixin Jin, MD**[5], **Renate Jerecic, PhD**[5], **Chun Yuan, PhD**[6], and **Debiao Li, PhD**[7]

[1]Department of Radiology, Anzhen Hospital, Capital Medical University, Beijing, China

[2]Department of Cardiology, Anzhen Hospital, Capital Medical University, Beijing, China

[3]Department of Ultrasound, Anzhen Hospital, Capital Medical University, Beijing, China

[4]Siemens Mindit Magnetic Resonance, Siemens Healthcare, MR Collaboration NE Asia, Shenzhen China

[5]Siemens Limited China, Siemens Healthcare, MR Collaboration NE Asia, Shanghai China

[6]Department of Radiology, University of Washington, Seattle, Washington, USA

[7]Biomedical Imaging Research Institute, Cedars-Sinai Medical Center, University of California, Los Angeles, California, USA

Abstract

Purpose—To evaluate the ability of black-blood coronary arterial wall MRI to identify the coronary artery plaque, using intravascular ultrasound (IVUS) as the golden standard.

Materials and Methods—Nineteen consecutive patients underwent IVUS and coronary artery wall MRI. Cross-sectional images were acquired on the lesion of coronary artery from the ostium to the middle segment continuously. The vessel cross-sectional area (CSA), luminal CSA, plaque burden, contrast-to-noise ratio (CNR) and signal-to-noise ratio (SNR) were measured in each slice which was then compared with the IVUS images.

Results—Sixteen of 19 patients completed coronary artery MRA and wall imaging. 41 of 67 slices were found plaques on both IVUS and MRI; The maximal wall thickness, plaque burden, SNR, CNR in the coronary wall containing plaque were greater compared with the normal coronary wall (1.70 ± 0.51 versus 1.24 ± 0.24; 0.71 ± 0.13 versus 0.59 ± 0.12; 1.86 ± 0.41 versus 1.47 ± 0.23; 5.10 ± 2.21 versus 2.99 ± 1.17; respectively, $P < 0.05$). The matched MRI and IVUS showed good correlation for vessel CSA (16.77 ± 10.67 versus 16.97 ± 8.36; r = 0.79; $P < 0.01$), luminal CSA (5.18 ± 5.01 versus 7.13 ± 5.14; r = 0.88; $P < 0.01$), plaque burden (0.71 ± 0.13 versus 0.59 ± 0.15; r = 0.67; $P < 0.01$). in segments containing plaques, especially the luminal CSA were strongly correlated.

© 2011 Wiley Periodicals, Inc.

[*]Address reprint requests to: Z.Z., Department of Radiology, No 2, Anzhen Road, Chaoyang District, Beijing, China. zhaoqi5000@vip.sohu.com.

NIH-PA Author Manuscript
NIH-PA Author Manuscript
NIH-PA Author Manuscript

NIH-PA Author Manuscript

NIH-PA Author Manuscript

NIH-PA Author Manuscript

Conclusion—MRI coronary artery wall imaging can identify coronary plaque in the proximal segments. It also has the potential to assess coronary artery size.

Keywords

MRI; coronary arteries; vessel wall; atherosclerosis; plaques

CLINICALLY SIGNIFICANT CORONARY artery disease (CAD) is typically defined as greater than 50% luminal diameter reduction. However, millions of people who experience sudden cardiac events (acute coronary syndromes and/or sudden cardiac death) secondary to coronary atherosclerosis each year have no significant CAD or prior symptoms. Plaque rupture is the most common complication of atherosclerosis, accounting for approximately 70% of fatal acute myocardial infarctions and/or sudden coronary deaths (1-3). Therefore, the ability to directly assess coronary artery endothelial injury, plaque composition, and positive remodeling has profound potential clinical impact. A prior detection of vulnerable plaques may allow early intervention, and reduce the occurrence of sudden cardiac events. However, x-ray coronary angiography, the current diagnostic reference for CAD, only assesses the vessel luminal diameter and does not provide direct information regarding coronary artery wall or atherosclerotic plaques.

Intravascular ultrasound (IVUS) imaging allows the simultaneously assessment of the lumen, vessel wall, and the atherosclerotic plaque. It is considered the reference method for visualizing the coronary artery wall (4). However, it is an invasive technique and is not appropriate for screening or serial examinations. Multidetector computed tomography (MDCT) is highly effective for noninvasive identification and quantification of calcified coronary plaques, but the accuracy for identifying noncalcifed plaque components such as lipid-rich (soft) or fibrotic components remains low. This due to the overlap of CT values of different composition in noncalcifed plaque (5,6). MRI has recently been shown to be a promising method of examining vessel wall thickness and detecting positive outward remodeling without obvious luminal narrowing in the coronary artery (7-9), but the accuracy of this approach has not been evaluated against the reference method. The purpose of this study was to evaluate the accuracy of black-blood coronary arterial wall MRI to identify and quantify coronary artery plaques by directly comparing with IVUS.

MATERIALS AND METHODS

Patient Recruitments

From October 2009 to April 2010, 19 consecutive patients (mean age 58 ± 9 years, 12 men) who were either scheduled for or had completed IVUS examination, but did not perform percutaneous coronary intervention (PCI), underwent coronary artery wall MRI within 10 days before or after IVUS examination. The indication of coronary artery angiography and IVUS were refer to the ACC guideline and the discretion of the cardiologists (10), Exclusion criteria included acute myocardial infarction within 2 weeks, unstable angina, heart rate above 80 beats/min (after giving β-blocker), arrhythmia, and any contraindications to MR examination (metallic implants such as pacemakers, defibrillators, cerebral aneurysm clips, severe claustrophobia). No clinical cardiac events were reported between the two

NIH-PA Author Manuscript

NIH-PA Author Manuscript

NIH-PA Author Manuscript

examinations. Written informed consent was obtained from each patient. The study was approved by the Ethics Committee of Beijing Anzhen Hospital.

MRI Protocol

All participants were imaged on a 1.5 Tesla (T) whole-body MR scanner (Sonata, Siemens, Erlangen, Germany) with a gradient strength of 40 mT/m, slew rate of 200 T/m/s, and 12-channel radiofrequency receive coils (6 anterior and 6 posterior) The R-wave acquired from a four-lead electrocardiogram (ECG) was used to trigger the data acquisition. An elastic belt was placed on the abdomen of the patient to avoid changes in depth of breathing during data acquisition. The 25–50 mg β-blocker (metoprolol tartrate tablets, China) was given orally to patients with heart rate >75 beats/min. All images were collected under free breathing with the patients in supine position.

A four-chamber cine scan was run first to determine the data acquisition window (DAW). Appropriate DAW was crucial for high-quality coronary MRA and wall imaging. A free breathing, retrospectively ECG-triggered steady state free precession (SSFP) sequence was used. The temporal resolution was 28 ms and spatial resolution was $2.2 \times 1.6 \times 6.0\ mm^3$. Whole-heart coronary MRA using DAW provided by cine imaging was acquired during free breathing to cover the entire coronary artery tree in one scan. The sequence was an ECG-triggered, navigator-gated, T2-prepared, segmented three-dimensional (3D) SSFP. Imaging parameters included: TR/TE = 3.4/1.7 ms, bandwidth flip angle = 890 Hz/pixel, angle =90°, voxel size = $0.7 \times 0.7 \times 0.9\ mm^3$ interpolated from $1.4 \times 1.4 \times 1.5\ mm^3$, navigator acceptance window = ± 2.5 mm.

Multiplanar reformations were performed on MRA images to show the left main coronary artery (LM), the proximal and middle left anterior descending artery (LAD), circumflex (LCX), and the right coronary artery (RCA). Image analysis of coronary MRA was quickly performed by two observers to detect luminal lesion. The lesion was defined as luminal diameter reduces or signal intensity decrease. Then 2D cross-sectional black-blood imaging was performed on the coronary artery (LM, LAD, LCX, or RCA) that had at least one lesion based on whole-heart coronary MRA. Contiguous images were acquired from the ostium to the middle segment without interval using DAW same as whole heart coronary MRA. Each cross-sectional image was individually prescribed based on double oblique multiplanar reformations to be orthogonal to the local longitudinal axis of the coronary wall. A double inversion recovery, ECG-triggered navigator-gated, fat suppressed, turbo spin echo (TSE) sequence was used with the following parameters: TR = 2 R–R intervals, TE = 31 ms, echo spacing = 6.1 ms, bandwidth = 303 Hz/pixel, echo train length = 13 acquisition matrix = 312 × 384, field of view = $325 \times 400\ mm^2$, in-plane resolution = $1.04 \times 1.04\ mm^2$, slice thickness = 5 mm, navigator acceptance window = ± 2.5 mm. Average = 1 the total examination time to complete the protocols was 60 min or less.

MRI Analysis

Coronary wall images were graded on a 3-point scale: 1 = invisible; 2 with = adequate; and 3 (7). Images a score of 2 or good 3 were analyzed using software (CASCADE) (11).

NIH-PA Author Manuscript

NIH-PA Author Manuscript

NIH-PA Author Manuscript

Coronary wall images were zoomed by a factor of 3. The outer (adventitial) and inner (luminal) boundaries of the coronary wall were traced manually using a region-of-interest (ROI) tool. The following parameters were measured: The outer contour area vessel cross-sectional area (vessel CSA), the inner contour area (luminal CSA), and percentage plaque burden, defined as vessel CSA minus luminal CSA divided by vessel CSA. An ROI tool was used to measure the signal intensity (SI). The area of ROI was 1.0 mm^2. The signal-to-noise ratio (SNR) was calculated based on the following formula: $SNR = SI_{wall} / SD_{noise}$, where SI of the vessel wall was determined by placing the ROI on the vessel wall, and the standard deviation (SD) of the background noise was determined from an ROI placed in the air anterior to the chest wall. Contrast-to-noise ratio (CNR) was calculated based on the following formula: $CNR = (SI_{wall} - SI_{perivascular}) / SD_{noise}$. For the purpose of determining the SI of the perivascular area, the ROI was placed in the region between the vessel wall and the myocardium.

Intravascular Ultrasound

IVUS was performed as part of the invasive diagnostic procedure using a commercial 40-MHz catheter (Atlantis Pro 2.9-F, Boston Scientific, Maple Grove, MN). The in-plane spatial resolution is 0.2 mm. After coronary angiography, IVUS examination was performed only in the branch with plaques. The IVUS catheter was positioned sufficiently distal (30 mm) to the targeted site, and auto pullback to the ostium of the branch at a speed of 0.5 mm/s was used. The IVUS data were stored digitally and assessed offline by the software (iReview, Boston Scientific).

IVUS Analysis

For comparison with MRI, the target coronary arteries were divided into 5-mm segments from the ostium or onset using the longitudinally reconstructed IVUS. Each 5-mm section was compared side by side with MRI. Furthermore, we selected side branches as fiduciary points to ensure that the same corresponding coronary sections were compared. Each 5-mm section in IVUS was then divided into five 1-mm sections; we used the average value of the five sections for comparison with MRI. The external elastic membrane (EEM) CSA (equal to the vessel CSA in MRI), luminal CSA, and plaque burden were calculated after the borders of vessel intima and adventitia were depicted manually in each detectable cross section. At sites where extensive calcification or large side branches originate, if acoustic shadowing involved a relatively small arc (<90°), planimetry of the circumference was performed by extrapolation from the closest identifiable EEM borders, although measurement accuracy and reproducibility was reduced. If calcification was more extensive than 90° of the arc, EEM measurements would not be reported. These quantitative measurements were performed in accordance with the IVUS interpretation recommendations of the American College of Cardiology (ACC) (12) According to the ACC recommendations. Atherosclerotic plaques will be defined as lesions located between the media and the intima with a thickness of at least 0.5 mm.

Two investigators independently determined the presence or quantitative measurements of atherosclerotic plaques in both IVUS and MRI images.

NIH-PA Author Manuscript

NIH-PA Author Manuscript

NIH-PA Author Manuscript

Statistical Analysis

Statistical analyses were performed with software SPSS13.0. Continuous variables were presented as means and standard deviations. An unpaired t test was performed to evaluate differences between plaque and normal wall thickness (divided by IVUS) in MRI. For comparison of the external elastic membrane CSA, luminal CSA, and plaque burden obtained by MRI and IVUS, the Pearman's correlation coefficient was determined. *P*-values of <0.05 were considered statistically significant.

RESULTS

Participant Characteristics

The characteristics of the study population are summarized in Table 1. Sixteen patients completed coronary artery MRA and wall imaging (84%), 3 patients were excluded from analysis (16%) (2 were due to poor MR image quality; 1 was due to premature ventricular contraction during the examination). The mean heart rate was 67.08 ± 8.35 beats/min. The mean navigator efficiency of whole heart MRcoronary imaging was 36 ± 11% (min 16%, max 56%), the average scan time were 11.2 ± 4.1 min (min 4.9 min, max 23.1 min). The mean navigator efficiency of wall imaging was 41 ± 12% (min 20%, max 70%). The average scan time was 2.1 ± 0.9 min (min 0.9 min, max 4.0 min) for each slice.

Image Quality

The image quality of MRA was adequate for analysis at the sites where coronary artery wall images were obtained in all 16 participants who completed the study. Five slices were excluded because of severe calcify in IVUS. Finally, a total of 67/82 (81%) coronary wall MR images with image quality scores 2 or 3 in the 16 participants (1 RCA, 15 LAD) were analyzed. Fifteen slices were excluded because of poor image quality (n = 3), small diameter (n = 8), or located in bifurcation (n = 4). The image quality of coronary artery wall imaging is summarized in Table 2. The assessable rates in LM (78.6%) and proximal segment of LAD (89.7%) were substantially higher than that of the middle segment of LAD (55.6%). The weighted kappa value for interobserver agreement for image quality grading was 0.79.

Accuracy of Coronary Artery Wall Imaging

Plaques were found in 41/67 slices in both IVUS and MRI. In MRI, the maximal wall thickness, plaque burden, SNR, and CNR in the coronary wall containing plaques were greater than those of the normal coronary wall (1.70 ± 0.51 versus 1.24 ± 0.24; 0.71 ± 0.13 versus 0.57 ± 0.11; 1.86 ± 0.40 versus 1.46 ± 0.22; 5.10 ± 2.21 versus 2.99 ± 1.17, respectively, $P < 0.01$). In all sites, the matched MRI and IVUS showed moderate correlation for vessel CSA (15.94 ± 9.75 versus 16.64 ± 7.88; r = 0.79 $P < 0.01$), luminal CSA (5.57 ± 4.53 versus 8.46 ± 5.67; r = 0.74; $P < 0.01$), and plaque burden (0.65 ± 0.14 versus 0.54 ± 0.20; r = 0.58; $P < 0.01$). The difference between the 2 correlations was statistically significant ($P < 0.001$). Only in slices containing plaques, the vessel CSA (16.77 ± 10.67 versus 16.97 ± 8.36; r = 0.79; $P < 0.01$), luminal CSA (5.18 ± 5.01 versus 7.13 ± 5.14; r = 0.88; $P < 0.01$), and plaque burden (0.71 ± 0.13 versus 0.59 ± 0.15; r = 0.67; $P < 0.01$) measured by MRI and IVUS were better correlated, especially the luminal CSA was

NIH-PA Author Manuscript

NIH-PA Author Manuscript

NIH-PA Author Manuscript

strongly correlated (Fig. 1). Comparison plots of vessel CSA, lumen CSA, and plaque burden of only the plaque sites and all sites between MRI and IVUS as well as scatter plot were shown in Figure 2 and Figure 3, respectively.

DISCUSSION

In this study, the accuracy of coronary artery wall imaging to identify the coronary artery plaque was evaluated using IVUS as the reference. We used a 2D double inversion recovery-prepared, ECG-triggered, navigator-gated, fat suppressed turbo spin-echo sequence to acquire cross-sectional coronary artery wall images. We can obtain excellent MR images in LM, proximal segment of LAD, proximal and middle segments of RCA (only one RCA). Because of the limitation of our technique, the image quality distal to the proximal segment of LAD was markedly decreased. In coronary wall imaging containing plaques, the plaque burden, SNR, and CNR were significantly higher than those of the normal coronary walls, which suggest that coronary artery cross-sectional wall imaging could identify coronary artery plaques from normal walls. Good correlation between MRI and IVUS was found for vessel CSA, lumen CSA, and plaque burden measurements, especially in the sites containing plaques. Although MRI overestimated the plaque burden and the degree of lumen stenosis, it has the potential to evaluate coronary artery size.

Previous studies have examined the ability of black blood MRI in identifying coronary artery wall thickening. Fayad et al (13) and Botnar et al (14) used 2D black-blood MRI to evaluate coronary arteries in normal participants and patients. The results showed that the average maximum coronary wall thickness in patients was significantly greater than that in normal participants. Another report by Kim et al (15) used 3D black-blood coronary wall MRI to detect positive arterial remodeling in the RCA of 6 patients in areas of nonsignificant CAD (10% to 50% diameter reduction). Both mean coronary wall thickness and wall area were significantly increased in patients compared with 6 healthy participants, whereas the lumen diameter and lumen area were similar, indicating positive arterial remodeling. In the present study, we used IVUS as the reference method, accurately dividing the normal and plaque segments. It was shown that the plaque burden was significantly higher in the slices containing plaques, which suggests that it is possible to identify plaques based on the morphology information. Meanwhile, in coronary walls containing plaques, the SNR and CNR were significantly higher than those in the normal coronary walls, which provide further evidence that MRI can be used to identify plaques. The increases in SNR and CNR in segments containing plaques maybe correlated with the wall thickening, lipid, and hemorrhage in the plaque.

Our study showed there was a good agreement between IVUS and MRI in vessel CSA, lumen CSA, and plaque burden, especially in segments containing plaques. This result suggests that MRI could evaluate coronary artery plaques and lumen stenosis on relative terms, which provide further basis for screening coronary artery disease by MRI. This technique could be used to improve coronary artery disease detection with bright-blood coronary MRA (16). However, MRI overestimated the severity of stenosis and plaque burden. The overestimation may be explained by the lower in-plane (1×1 mm^2) and through-plane spatial resolution (5 mm) of MRI compared with IVUS. It would lead to

NIH-PA Author Manuscript

NIH-PA Author Manuscript

NIH-PA Author Manuscript

partial volume effect resulting in an overestimation of the true vessel wall area and thickness. In areas of normal vessel wall, partial volume effect is more severe because the wall is thinner, which might explain the reason why the correlation between the two modalities in areas of plaque were greater. Furthermore, residual respiratory or cardiac motion may cause image blurring, thereby leading to an overestimation of the true vessel wall area. Compared with MRI, IVUS vessel wall measurements do not include the adventitia, which might also contribute to the larger coronary vessel wall areas as measured by MRI.

Cross-sectional imaging of the coronary arteries is challenging because of their complex anatomical geometry, small size, and 3D rapid movement. An assessable coronary artery wall imaging based on good compensation of cardiac and respiration movement, suppression of the surrounding tissues include myocardium and fat to clearly delineate outer boundaries of the vessel, suppression of the blood signal in the coronary artery to identify the inner wall (17,18). In our study, we could analyze most LM and proximal LAD segments, but nearly half of the distal segments were nonassessable. The reason maybe includes two points, first, the diameter of the vessel is too small, and the partial volume effects affect the delineation of real vessel wall. Another reason is that the middle segment of coronary arteries are very close to the myocardium, absent of adjacent periadventitial fat, however, the present technique could not differentiate the myocardium and the outer wall of vessel.

Several important limitations exist in the current study. First, the scan time was relatively long. Two patients could not tolerate the long scan time, the state of respiratory and heart rate became unstable, the image quality was poor, and finally they withdrew from the study. Scan time was dependent on respiratory gating efficiency and heart rate. With prolonged scan time, the patients' breathing patterns and heart rates tended to vary, which could reduce the image quality. The average duration for each imaging session was approximately 60 min. Faster imaging techniques such as parallel data acquisition with higher acceleration factors should allow further improvement in imaging speed. Second, the spatial resolution of MRI was worse than intravascular ultrasound, which caused MRI to overestimate the plaque burden. Higher field imaging may allow further increased spatial resolution (19,20). Third, due to the thin vessel wall, the value of SNR and CNR may affected by the limited number of pixels and by partial valuing. Fourth, only one weighted imaging was used in the present study, limiting its ability to analyze the plaque composition. A combination of T1-weighted (21-23), T2-weighted, and contrast-enhanced imaging may alleviate this problem.

In conclusion, MRI coronary artery wall imaging can identify plaques in proximal segments of the coronary artery. Good correlation was found between MRI and IVUS, which suggests that MR vessel wall imaging can relatively assess plaque burden and lumen stenosis. Future work will certainly aim at the improvements in resolution, image quality and the identification of the different plaque components.

Acknowledgments

Contract grant sponsor: National Natural Science Foundation of China; Contract grant sponsor: Projects of International Science Technology Cooperation and Exchanges; Contract grant numbers: 30870733, S2010BR0551.

NIH-PA Author Manuscript

NIH-PA Author Manuscript

NIH-PA Author Manuscript

REFERENCES

1. Naghavi M, Libby P, Falk E, et al. From vulnerable plaque to vulnerable patient a call for new definitions and risk assessment strategies: part I. Circulation. 2003; 108:1664–1672. [PubMed: 14530185]
2. Lloyd-Jones D, Adams R, Carnethon M, et al. Heart disease and stroke statistics - 2009 update: a report from the American Heart Association Statistics Committee and Stroke Statistics Subcommittee. Circulation. 2009; 119:480–486. [PubMed: 19171871]
3. Falk E, Shah PK, Fuster V. Coronary plaque disruption. Circulation. 1995; 92:657–671. [PubMed: 7634481]
4. Ge J, Chirillo F, Schwedtmann J, et al. Screening of ruptured plaques in patients with coronary artery disease by intravascular ultrasound. Heart. 1999; 81:621–627. [PubMed: 10336922]
5. Sun J, Zhang Z, Lu B, et al. Identification and quantification of coronary atherosclerotic plaques: a comparison of 64-MDCT and intravascular ultrasound. AJR Am J Roentgenol. 2008; 190:1–7.
6. Motoyama S, Kondo T, Sarai M, et al. Multislice computed tomographic characteristics of coronary lesions in acute coronary syndromes. J Am Coll Cardiol. 2007; 50:319–326. [PubMed: 17659199]
7. Miao C, Chen S, Macedo R, et al. Positive remodeling of the coronary arteries detected by magnetic resonance imaging in an asymptomatic population mesa (multi-ethnic study of atherosclerosis). J Am Coll Cardiol. 2009; 53:1708–1715. [PubMed: 19406347]
8. Macedo R, Chen S, Lai S, et al. MRI detects increased coronary wall thickness in asymptomatic individuals: the multi-ethnic study of atherosclerosis (MESA). J Magn Reson Imaging. 2008; 28:1108–1115. [PubMed: 18837001]
9. Kim WY, Astrup AS, Stuber M, et al. Subclinical coronary and aortic atherosclerosis detected by magnetic resonance imaging in type 1 diabetes with and without diabetic nephropathy. Circulation. 2007; 115:228–235. [PubMed: 17190865]
10. Scanlon PJ, Faxon DP, Audet AM, et al. ACC/AHA guidelines for coronary angiography: executive summary and recommendations: a report of the American College of Cardiology/ American Heart Association Task Force on Practice Guidelines (Committee on Coronary Angiography). Developed in collaboration with the Society for Cardiac Angiography and Interventions. Circulation. 1999; 99:2345–2357. [PubMed: 10226103]
11. Kerwin W, Xu D, Liu F, et al. Magnetic resonance imaging of carotid atherosclerosis:plaque analysis. Top Magn Reson Imaging. 2007; 18:371–378. [PubMed: 18025991]
12. Mintz GS, Nissen SE, Anderson WD, et al. American College of Cardiology clinical expert consensus document on standards for acquisition, measurement and reporting of intravascular ultrasound studies (IVUS). J Am Coll Cardiol. 2001; 37:1478–1492. [PubMed: 11300468]
13. Fayad ZA, Fuster V, Fallon JT, et al. Noninvasive in vivo human coronary artery lumen and wall imaging using black-blood magnetic resonance imaging. Circulation. 2000; 102:506–510. [PubMed: 10920061]
14. Botnar RM, Stuber M, Kissinger KV, Kim WY, Spuentrup E, Manning WJ. Noninvasive coronary vessel wall and plaque imaging with magnetic resonance imaging. Circulation. 2000; 102:2582–2587. [PubMed: 11085960]
15. Kim WY, Stuber M, Börnert P, Kissinger KV, Manning WJ, Botnar RM. Three-dimensional black-blood cardiac magnetic resonance coronary vessel wall imaging detects positive arterial remodeling in patients with nonsignificant coronary artery disease. Circulation. 2002; 106:296–299. [PubMed: 12119242]
16. Dai, Q.; Zhang, Z.; He, Y., et al. Diagnostic performance of non-contrast W-HCMRA combined with black-blood arterial wall imaging in patients with suspected coronary artery disease; Proceedings of the 19th Annual Meeting of ISMRM; Stockholm. 2010; abstract 661
17. Malayeri AA, Macedo R, Li D, et al. Coronary vessel wall evaluation by magnetic resonance imaging in the multi-ethnic study of atherosclerosis: determinants of image quality. J Comput Assist Tomogr. 2009; 33:1–7. [PubMed: 19188777]
18. Desai MY, Lai S, Barmet C, Weiss RG, Stuber M. Reproducibility of 3D free-breathing magnetic resonance coronary vessel wall imaging. Eur Heart J. 2005; 26:2320–2324. [PubMed: 15972291]

NIH-PA Author Manuscript

NIH-PA Author Manuscript

NIH-PA Author Manuscript

19. Koktzoglou I, Simonetti O, Li D. Coronary artery wall imaging: initial experience at 3 tesla. J Magn Reson Imaging. 2005; 21:128–132. [PubMed: 15666403]

20. Bansmann PM, Priest AN, Muellerleile K, et al. MRI of the coronary vessel wall at 3 t: comparison of radial and cartesian k-space sampling. AJR Am J Roentgenol. 2007; 188:70–74. [PubMed: 17179347]

21. Kawasaki T, Koga S, Koga N, et al. Characterization of hyperintense plaque with noncontrast T1-weighted cardiac magnetic resonance coronary plaque imaging comparison with multislice computed tomography and intravascular ultrasound. JACC Cardiovascular Imaging. 2009; 2:720–728. [PubMed: 19520342]

22. Yeon SB, Sabir A, Clouse M, et al. Delayed-enhancement cardiovascular magnetic resonance coronary artery wall imaging comparison with multislice computed tomography and quantitative coronary angiography. J Am Coll Cardiol. 2007; 50:441–447. [PubMed: 17662397]

23. Maintz D, Ozgun M, Hoffmeier A, et al. Selective coronary artery plaque visualization and differentiation by contrast-enhanced inversion prepared MRI. Eur Heart J. 2006; 27:1732–1736. [PubMed: 16787955]

NIH-PA Author Manuscript

NIH-PA Author Manuscript

NIH-PA Author Manuscript

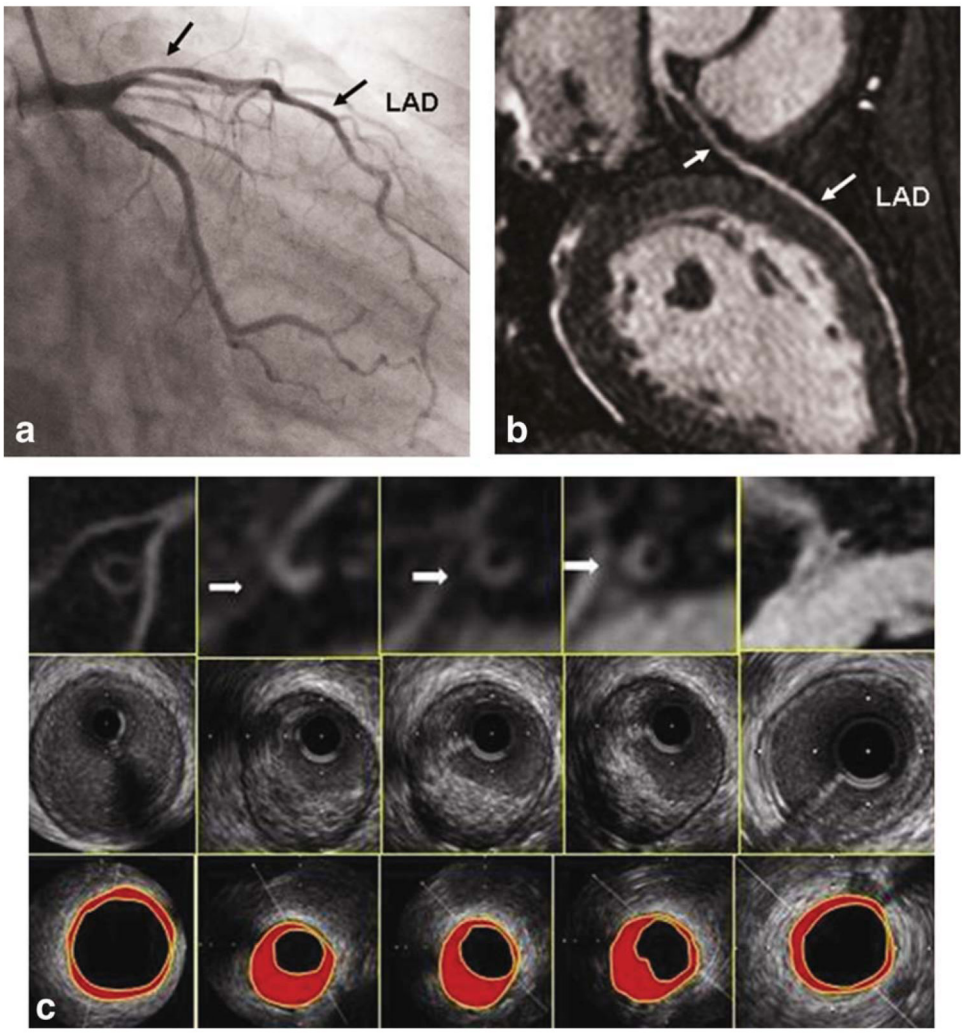

Figure 1.

A 46-year-old male participant with eccentric coronary plaque. **a:** LAD MRA showing moderate stenosis in the proximal coronary artery (left arrow). **b:** Conventional coronary artery angiography also shows moderate lumen stenosis in the same site (left arrow). **c:** Cross-sectional MRI coronary wall images (top row), corresponding IVUS images (middle row), and IVUS images (bottom row) from LM (right) to proximal segment of LAD (left). Plaques were found in MRI (arrows), which were correlated well with IVUS.

NIH-PA Author Manuscript
NIH-PA Author Manuscript
NIH-PA Author Manuscript

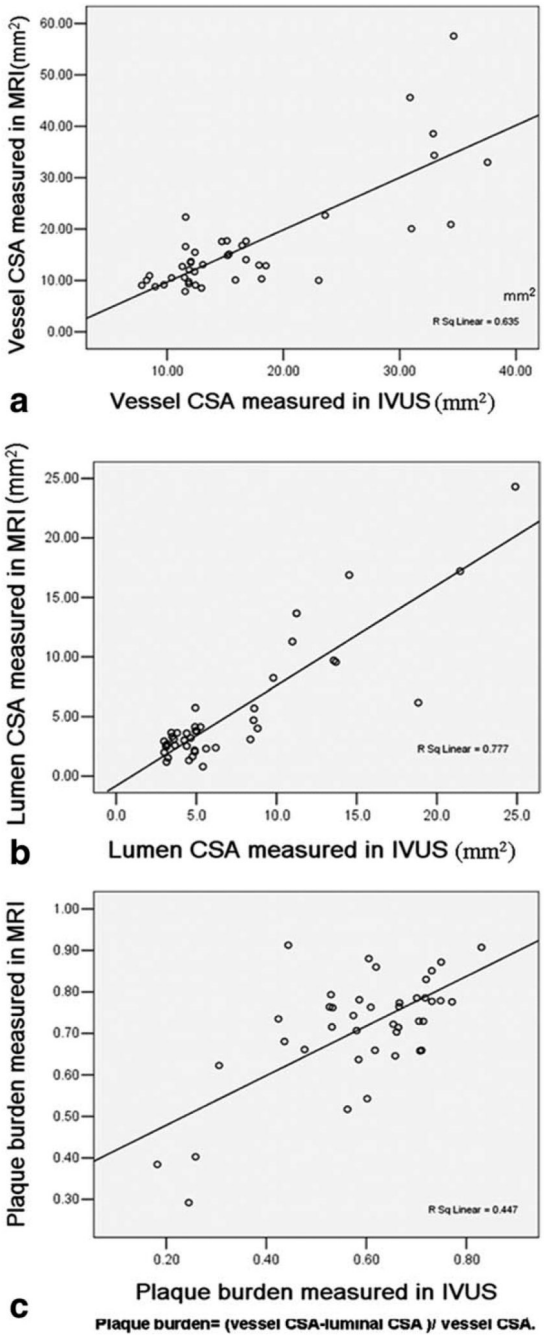

Figure 2.

Scatter plots of the vessel CSA **(a)**, lumen CSA **(b)**, and plaque burden **(c)** between MRI and IVUS in the sites containing plaques. The vessel CSA, lumen CSA, and plaque burden are positively correlated between MRI and IVUS. The measurements by MRI and IVUS are, respectively: the vessel CSA (16.77 ± 10.67 versus 16.97 ± 8.36; r = 0.79; $P < 0.01$), lumen CSA (5.18 ± 5.01 versus 7.13 ± 5.14; r = 0.88; $P < 0.01$), and plaque burden (0.71 ± 0.13 versus 0.59 ± 0.15; r = 0.67; $P < 0.01$).

NIH-PA Author Manuscript

NIH-PA Author Manuscript

NIH-PA Author Manuscript

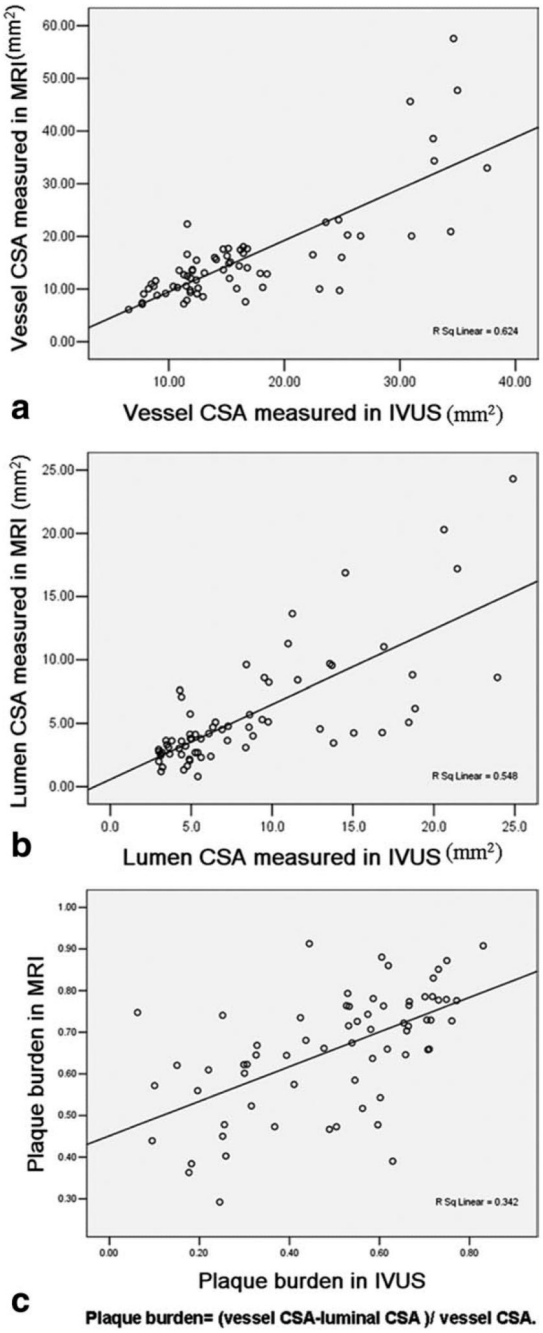

Figure 3.

Scatter plots of the vessel CSA **(a)**, lumen CSA **(b)**, and plaque burden **(c)** between MRI and IVUS in all slices. The vessel CSA, lumen CSA, and plaque burden are positively correlated between MRI and IVUS. The measurements by MRI and IVUS are, respectively: the vessel CSA (15.94 ± 9.75 versus 16.64 ± 7.88; r = 0.79 $P < 0.01$); lumen CSA (5.57 ± 4.53 versus 8.46 ± 5.67; r = 0.74; $P < 0.01$), and plaque burden (0.65 ± 0.14 versus 0.54 ± 0.20; r = 0.58; $P < 0.01$).

NIH-PA Author Manuscript

NIH-PA Author Manuscript

NIH-PA Author Manuscript

Table 1

Participant Characteristics

Total no. of patients	**19**
Age (years)	58 ± 9
Male patients, N (%)	12 (63.2%)
Hypertension, N (%)	10 (52.6%)
Diabetes, N (%)	5 (26.3%)
Hypercholesterol, N (%)	5 (26.4%)
Smoker, N (%)	8 (42.1%)
Chest pain, N (%)	15 (78.9%)
Family history, N (%)	5 (26.3%)
Mean heart rate (beats/min)	67.08 ± 8.35

NIH-PA Author Manuscript

NIH-PA Author Manuscript

NIH-PA Author Manuscript

Table 2

Image Quality of 82 Slices in 16 Patients

			Cause of non-assessable segments			
Artery	**No. of slices**	**Assessable slices (%)**	**Poor quality**	**Small diameter**	**Located at bifurcation**	**Mean score**
LM	14	12 (85.7%)	1		2	2.21 ± 0.80
LAD						
Proximal	39	35 (89.7%)	1	3		2.49 ± 0.68
Middle	18	10 (55.5%)	1	5	2	2.06 ± 0.99
RCA						
Proximal	2	2				3.00
Middle	9	9				2.33 ± 0.17